

NASA TECHNICAL NOTE

NASA TN D-8368



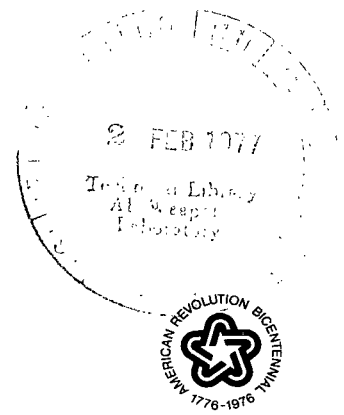
NASA TN D-8368 c.1

LOAN COPY: RE
AFWL TECHNICAL
KIRTLAND AFB



A NONLINEAR THEORY FOR AIRFOILS
WITH TRAILING-EDGE JET FLAP

Raymond L. Barger
Langley Research Center
Hampton, Va. 23665





0134106

1. Report No. NASA TN D-8368		2. Government Accession No.		3. Recipient's Catalog No.	
4. Title and Subtitle A NONLINEAR THEORY FOR AIRFOILS WITH TRAILING-EDGE JET FLAP		5. Report Date December 1976		6. Performing Organization Code	
7. Author(s) Raymond L. Barger		8. Performing Organization Report No. L-11126		10. Work Unit No. 505-06-31-02	
9. Performing Organization Name and Address NASA Langley Research Center Hampton, VA 23665		11. Contract or Grant No.		13. Type of Report and Period Covered Technical Note	
12. Sponsoring Agency Name and Address National Aeronautics and Space Administration Washington, DC 20546		14. Sponsoring Agency Code			
15. Supplementary Notes					
16. Abstract A nonlinear procedure for computing the pressure distribution on an airfoil with a trailing-edge jet flap is described. The method is not restricted to thin airfoils or shallow jet-deflection angles. Correlation with experiment indicates that the characteristics of the pressure distribution are predicted by the theory, but the effect of entrainment is overpredicted with the entrainment coefficient used.					
17. Key Words (Suggested by Author(s)) Airfoil Jet flap High lift Jet entrainment			18. Distribution Statement Unclassified - Unlimited Subject Category 02		
19. Security Classif. (of this report) Unclassified		20. Security Classif. (of this page) Unclassified		21. No. of Pages 15	
				22. Price* \$3.25	

A NONLINEAR THEORY FOR AIRFOILS WITH TRAILING-EDGE JET FLAP

Raymond L. Barger
Langley Research Center

SUMMARY

A nonlinear procedure for computing the pressure distribution on an airfoil with a trailing-edge jet flap is described. The method is not restricted to thin airfoils or shallow jet-deflection angles. Correlation with experiment indicates that the characteristics of the pressure distribution are predicted by the theory, but the effect of entrainment is overpredicted with the entrainment coefficient used.

INTRODUCTION

Interest in the jet flap stems from its effectiveness as a propulsive lift mechanism. A system, such as the jet flap, that increases the airfoil circulation is much more efficient than a pure jet reaction device.

Theoretical studies of jet-flap airfoils have special importance because of the difficulties involved in wind-tunnel tests on such complex devices. The initial theory for an airfoil with a jet flap was developed by Spence (ref. 1) who used thin-airfoil calculations together with thickness corrections obtained from transformation theory. The effect of jet vorticity was calculated by distributing vortices along the X-axis (consistent with thin-airfoil theory). Comparison with experiment indicated better agreement for the lift coefficient than for the pressure distribution because of compensating errors in the upper and lower surface pressures.

Spence did not treat the effects of jet entrainment, but such effects have been considered by Wagnanski in reference 2. Wagnanski also used a thin-airfoil analysis, with the symmetric airfoil at zero incidence represented as a straight-line segment, and the jet by a line of sinks extending downstream from the airfoil on the X-axis.

The present treatment includes the effects of both the jet deflection and the entrainment. The thin-airfoil assumptions are dropped so that arbitrary airfoil shapes and deflection angles are permitted. Boundary-layer effects are not included.

SYMBOLS

A_n, B_n	Fourier coefficients
a	length parameter used in transformation of airfoil to approximate circle
C_j	jet-momentum coefficient
C_M	jet mass flow coefficient, $\frac{\rho V \delta}{\frac{1}{2} \rho_{\infty} U_{\infty} c}$
C_p	pressure coefficient
c	chord length (assumed unity in calculations)
Im	imaginary part of complex quantity
i	imaginary unit
m_1	jet slope at airfoil trailing edge, $\tan \tau$
n	index
R	radius of circle into which airfoil is transformed
Re	real part of complex quantity
r	radial coordinate in z' -plane
S_j	sink strength in main region of jet
S_k	sink strength associated with k th jet segment
S_m	sink strength in mixing region of jet
s	distance along jet
U	local flow velocity in jet direction
V	jet velocity
W	complex velocity potential

w	conjugate of complex velocity
w_p	value of w in circle plane excluding contribution due to supercirculation
w_q	$= -\frac{i}{2\pi z}$
w_t	total value of w in circle plane
x, y	Cartesian coordinates in airfoil plane
z	complex variable representing points in circle plane
z'	complex variable representing points in near-circle plane
Γ_j	vortex strength representing supercirculation due to jet sheet
Γ_k	strength of vortex located in k th segment of jet sheet
Γ_ℓ	vortex strength associated with camber and angle of attack
γ	vorticity
δ	jet-slot width
ξ	complex variable representing points in airfoil plane
θ	angular coordinate in z' -plane
κ	curvature of jet sheet
ρ	density
σ	empirical parameter used in computing entrainment coefficient
τ	jet-deflection angle
ϕ	angular coordinate in circle plane
ψ	defined by relation $r = ae^\psi$

ψ_0 average value of ψ

Subscripts:

a airfoil plane

c circle plane

E due to entrainment

j jet

∞ free-stream conditions

Bar over a symbol denotes complex conjugate.

ANALYSIS

Transformation of Airfoil Into Circle

The first step in the analysis is to transform the airfoil into a circle by the method of Theodorsen (ref. 3). This method uses two consecutive mappings. The first is the Joukowski transformation

$$\zeta = z' + \frac{a^2}{z'} \quad (1)$$

which maps the airfoil in the ζ -plane into a contour approximating a circle in the z' -plane (fig. 1). The parameter a is determined so that if the airfoil is an ellipse of any thickness ratio, the mapped contour is an exact circle. (See ref. 3.)

The complex variable z' is now written in polar coordinates

$$z' = re^{i\theta}$$

and a new variable ψ is defined by

$$r = ae^{\psi}$$

so that

$$z' = ae^{\psi+i\theta}$$

Then the mapping of the contour to an exact circle in the z -plane (fig. 1) is accomplished by the relation

$$z' = ze^{\sum (A_n + iB_n)/z^n} \quad (2)$$

where A_n and B_n are R^n times the Fourier cosine and sine coefficients, respectively, of the function $\psi(\theta)$, which is obtained directly from the first (Joukowski) transformation. The radius R of the circle to which the airfoil is mapped is computed from the formula

$$R = ae^{\psi_0}$$

where ψ_0 is the average value of ψ .

Reference 3 demonstrates that relations (1) and (2) map points on the airfoil into points on the circle in the z -plane. However, since equation (2) is not analytically invertible, points that are not on the airfoil are not easily mapped into the z -plane, and some iteration is required. The iteration procedure, however, is simple and rapidly convergent.

On the other hand, the mapping of points from the circle plane to the airfoil plane is a straightforward process. Furthermore, velocities computed in the circle plane are simply converted to velocities in the airfoil plane by the relation

$$\left| \frac{dW}{d\xi} \right| = \left| \frac{dW}{dz} \right| \left| \frac{dz}{d\xi} \right|$$

with $\frac{d\xi}{dz}$ given by differentiation of equations (1) and (2):

$$\frac{d\xi}{dz} = \frac{d\xi}{dz'} \frac{dz'}{dz} = \frac{1}{z'} \left(z' - \frac{a^2}{z'} \right) z' \left(\frac{1}{z} + \frac{d}{dz} \sum \frac{A_n + iB_n}{z^n} \right) = z' - \frac{a^2}{z'} \left(\frac{1}{z} - \sum n \frac{A_n + iB_n}{z^{n+1}} \right)$$

Modeling the Jet Sheet

To determine the shape of the jet and the circulation that results from the jet deflection, the jet is modeled as a vortex sheet. The derivation of the required formulas is given in reference 1. The known quantities are the jet-deflection angle τ at the airfoil trailing edge and the jet-momentum coefficient

$$C_j = \frac{\rho V^2 \delta}{\frac{1}{2} \rho_\infty U_\infty^2 c}$$

The shape of the vortex sheet and the distribution of vorticity along the sheet are to be determined so that

(1) The boundary condition on the airfoil surface is satisfied.

(2) The vortex sheet has the given deflection τ at the trailing edge.

(3) The curvature of the jet sheet is consistent with the distribution of vorticity along the sheet; that is, the relation $\gamma = \frac{U_\infty^2 C_j \kappa}{2U}$ must be satisfied, where γ and κ are the local vorticity and curvature, respectively.

An iterative procedure is required for calculating the jet shape and the vorticity distribution so as to meet all these conditions simultaneously. The jet sheet is approximated in the circle plane as a set of straight-line segments of equal length Δs_c (see fig. 1). The first segment is determined so that the corresponding line in the airfoil plane has the given jet-deflection angle. For the first iteration, the remaining segments are chosen arbitrarily so that the slopes decrease exponentially with distance s along the jet. Then the vertex locations are determined, each point from the previous one, starting at the trailing edge. By moving the distance of one segment length in the direction specified by the slope for that segment, the location of the next point is determined. The curvature distribution is also simply determined since the change in angle $\Delta\theta$ at each vertex can be obtained from the slopes of the adjacent segments and the segment lengths are equal. Thus, the curvature $\frac{\Delta\theta}{\Delta s}$ can be calculated directly. A vortex is located at the center of each of the segments.

Now consider the representation of the jet sheet in the airfoil plane. This jet sheet consists of an equal number of segments, but the segments are not of equal length. The first segment has the direction specified by the given value of τ . A vortex is located on each segment with a strength determined by the approximation

$$\Gamma_a = \gamma_a \Delta s_a = \frac{1}{2} \frac{U_\infty^2}{U_a} \frac{\Delta\theta_a}{\Delta s_a} \Delta s_a = \frac{1}{2} \frac{U_\infty^2}{U_a} \Delta\theta_a$$

where $\Delta\theta_a$ is the average change in angle at the vortex and is determined by the average change in angle at the adjacent vertices. Since the mapping is conformal at each

vertex (although it is generally not conformal at the initial point located at the trailing edge), the change in angle is the same as the change in angle at the corresponding vertex in the circle plane. Thus,

$$\Delta\theta_a = \Delta\theta_c$$

In general, it is not true that $U_a = U_c$, but for all cases calculated, U_a differed so slightly from U_c at the vortex locations that the adjustment in Γ because of the difference between U_a and U_c was essentially negligible. Therefore, the approximation

$$\Gamma_a = \frac{1}{2} \frac{U_\infty^2}{U_c} \Delta\theta_c \quad (3)$$

was adopted. This approximation shortens the calculation significantly as it permits the iteration to be carried out entirely in the circle plane.

The iteration procedure requires the calculation of the velocity vector at each vortex location. The velocity equation in the circle plane is

$$\frac{dw}{dz} = -U_\infty \left(1 - \frac{R^2}{z^2} - \frac{i(\Gamma_\ell + \Gamma_j)}{2\pi z} - \frac{i}{2\pi} \sum_k \left(\frac{\Gamma_k}{z - z_k} - \frac{\Gamma_k}{z - \frac{R^2}{\bar{z}_k}} \right) \right) \quad (4)$$

where the terms, in order, represent the undisturbed free stream, the doublet effect of the circle, the vortex due to the circulation associated with camber and angle of attack, the additional vortex associated with airfoil circulation resulting from the presence of the jet sheet, the vortices representing the jet sheet, and their images in the circle. Here, $\frac{dw}{dz}$ actually denotes the complex conjugate of the velocity variable.

On each iteration, the calculation requires several steps. First, the vortex strengths Γ_k are determined by applying equation (3) at the k th segment. Then, since Γ_ℓ is known (see ref. 3), the only remaining parameter to be determined in the velocity equation is the "supercirculation" Γ_j . This quantity is obtained from the condition that the first segment of the vortex sheet must have the direction specified by the given jet-deflection angle. The velocity at the center of the first segment can be written

$$w_T = w_p + \Gamma_j w_q \quad (5)$$

where $w_q = -\frac{i}{2\pi z}$, and w_p denotes all the remaining terms on the right side of equation (4). Since w_T is the complex conjugate of the velocity variable, the relation

$$m_1 \equiv \tan \tau = -\frac{\text{Im}(w_T)}{\text{Re}(w_T)} \quad (6)$$

must be satisfied. Substituting from equation (5) into equation (6) and solving for Γ_j yields

$$\Gamma_j = -\frac{\text{Im}(w_p) + m_1 \text{Re}(w_p)}{\text{Im}(w_q) + m_1 \text{Re}(w_p)}$$

With this value of Γ_j , the velocity vector can be computed at the center of each segment of the jet sheet; thereby the slope of each segment is fixed. This distribution of slopes is summed to obtain the jet shape for the next iteration, and it is differenced to obtain the curvature. Then, the curvature and the magnitude of the velocity are used to obtain the distribution of vortex strengths for the next iteration by means of equation (3).

Considerable care is required in setting up the iterative calculation because of the dependence of the velocity on the curvature of the jet sheet. Any slight "kink" in the sheet arising in the calculation denotes an abnormally high local curvature and thus tends to trigger an instability leading to divergence. Approximating the sheet with polynomial or trigonometric series is not practical because increasing the accuracy of the approximation in the least-squares sense requires increasing the number of terms, thereby increasing the number of "wiggles" in the shape, and causing large local values of curvature. A spline fit generally results in even larger curvature variations.

The smoothing process that was adopted used a smooth analytic shape on the first iteration. The results of each subsequent iteration were averaged with those of the previous iteration. This procedure proved satisfactory for values of C_j up to three. For larger values of C_j , it was necessary to start at three and gradually increase C_j during the iteration process. The convergence criterion adopted was that the value of Γ_j must vary less than 0.5 percent between successive iterations. The number of iterative cycles required has varied from 6 to 16 in the examples studied.

The problem of convergence of the jet shape would probably be reduced if the vorticity were distributed over each segment rather than concentrated at a single vortex at the midpoint of the segment.

Velocity Due to Jet-Entrainment Effect

After the jet shape has been established, one can compute the entrainment effect by distributing sinks along the jet. Formulas for the sink strengths per unit length, as given in reference 2, are

$$S_m = 0.064(V - U_\infty) \quad (7)$$

for the initial mixing region of the jet, and

$$S_j = U_\infty \left[\frac{3(C_j - C_M)}{8\sigma(\delta/c)} \right]^{1/2} \quad (8)$$

for the main region of the jet, where the velocity profile is self-similar. These formulas are derived for a two-dimensional jet in a uniform free stream parallel to the jet axis, but some experimental results quoted in reference 2 indicate that they also represent a good approximation for an inclined jet. The parameter σ is estimated to be 7.7 from experimental data (ref. 2). Since formulas (7) and (8) give the sink strength per unit distance along the jet, the actual strengths are determined by multiplying these values by the corresponding distances along the jet. A sink is located on each of the straight-line segments, and the strengths are determined in the airfoil plane. For each of these sinks, there is a sink of equal strength at the corresponding point in the circle plane (ref. 4, sec. 8.50). In the circle plane, the velocity due to entrainment can be computed by the circle theorem which gives

$$\left. \frac{dw}{dz} \right|_E = \sum \left(\frac{-S_k}{z - z_k} - \frac{S_k}{z - \frac{R^2}{\bar{z}_k}} + \frac{S_k}{z} \right)$$

Thus, the boundary condition is satisfied by including, in addition to each sink, the image of the sink in the circle and a source of equal strength at the origin. The velocity due to entrainment is computed on the circle and added to the previously computed velocity distribution.

It may be noted that the attempt to include the entrainment calculation in the iterative procedure for the jet shape is not practical because the jet sheet has to be represented as a distribution of vortices to obtain its shape, but it must be represented as a distribution of sinks to compute the entrainment effect.

Examples and Discussion

The potential advantage to be gained by the use of a jet flap is illustrated by the example shown in figure 2. For this example, the thickness ratio is 0.13, $C_j = 2.0$, and $\tau = 45^\circ$. One can see from the figure that the supercirculation due to the jet flap generates a large increase in lift. The effect of entrainment on the lower surface pressures tends to reduce the lift, but this effect is more than compensated for on the upper surface. The total increase in lift coefficient is about 500 percent, from 0.5 to approximately 2.5 percent.

The only example of a measured pressure distribution given in reference 1 is for a 12.5-percent thick ellipse with a jet-deflection angle of 31.4° . When the nonlinear theory without entrainment is compared with Spence's modified thin-airfoil theory for this case (fig. 3), the results of the two theories compare very closely over most of the airfoil. This similarity was to be expected inasmuch as the jet-deflection angle was small, the airfoil was relatively thin, and thickness correction factors were applied to the thin-airfoil results. The nonlinear theory is somewhat closer to the experimental results in the regions of high curvature near the trailing edge. For a more conventional airfoil shape, the Spence theory would compare even more closely if accurate thickness corrections could be made. However, since the full transformation is required to obtain accurate thickness corrections for a general airfoil shape, the entire nonlinear theory can be used with little more trouble. The advantages of the nonlinear theory would also increase with increasing thickness ratio and jet-deflection angle.

When the velocity due to entrainment is included in the nonlinear theory, virtually all the characteristics of the experimental pressure distribution are predicted qualitatively by the theory (fig. 3). However, the effect of the entrainment is overpredicted somewhat. This error may arise from the failure to account for the curvature of the jet in computing the entrainment coefficients or it may be associated with an error in the empirical parameter σ . In any case, if the entrainment coefficient is arbitrarily reduced by 40 percent, the correlation with experiment is much better for this particular example (fig. 4). The small discrepancy near the trailing edge on the lower surface results from the fact that the jet slot was located in the vicinity of the 98-percent station rather than at the trailing edge as assumed in the calculation.

CONCLUDING REMARKS

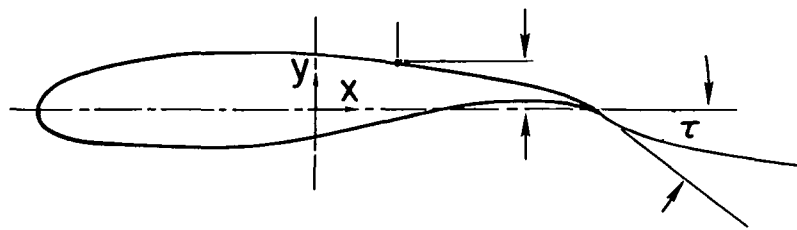
A nonlinear procedure for computing the pressure distribution on an airfoil with a trailing-edge jet flap has been described. The method is not restricted to thin airfoils or shallow jet-deflection angles. Correlation with experiment indicates that the

characteristics of the pressure distribution are predicted by the theory, but the effect of entrainment is overpredicted with the entrainment coefficient used.

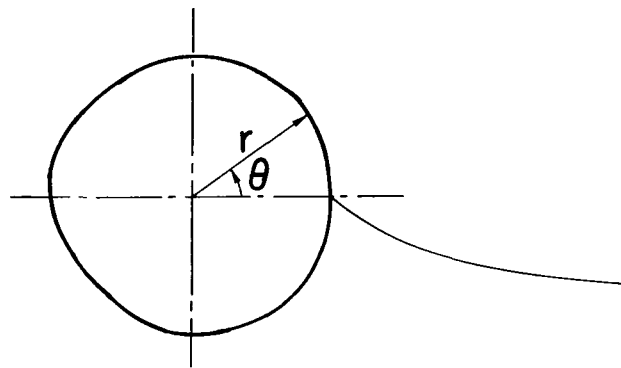
Langley Research Center
National Aeronautics and Space Administration
Hampton, VA 23665
November 19, 1976

REFERENCES

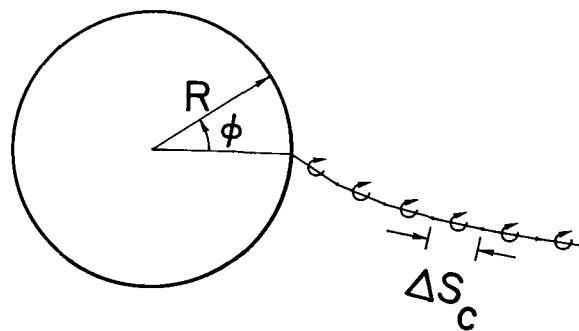
1. Spence, D. A.: The Lift Coefficient of a Thin, Jet-Flapped Wing. Proc. Roy. Soc. (London), ser. A, vol. 238, no. 1212, Dec. 4, 1956, pp. 46-68.
2. Wagnanski, I.: The Effect of Jet Entrainment on Loss of Thrust for a Two-Dimensional Symmetrical Jet-Flap Aerofoil. Aeronaut. Quart., vol. XVII, pt. 1, Feb. 1966, pp. 31-52.
3. Theodorsen, Theodore: Theory of Wing Sections of Arbitrary Shape. NACA Rep. 411, 1931.
4. Milne-Thomson, L. M.: Theoretical Hydrodynamics. Second ed. Macmillan Co., 1950.



(a) Airfoil or ζ -plane.



(b) Near-circle or z' -plane.



(c) Circle or z -plane.

Figure 1.- Representations of airfoil profile and trailing jet as used in calculations.

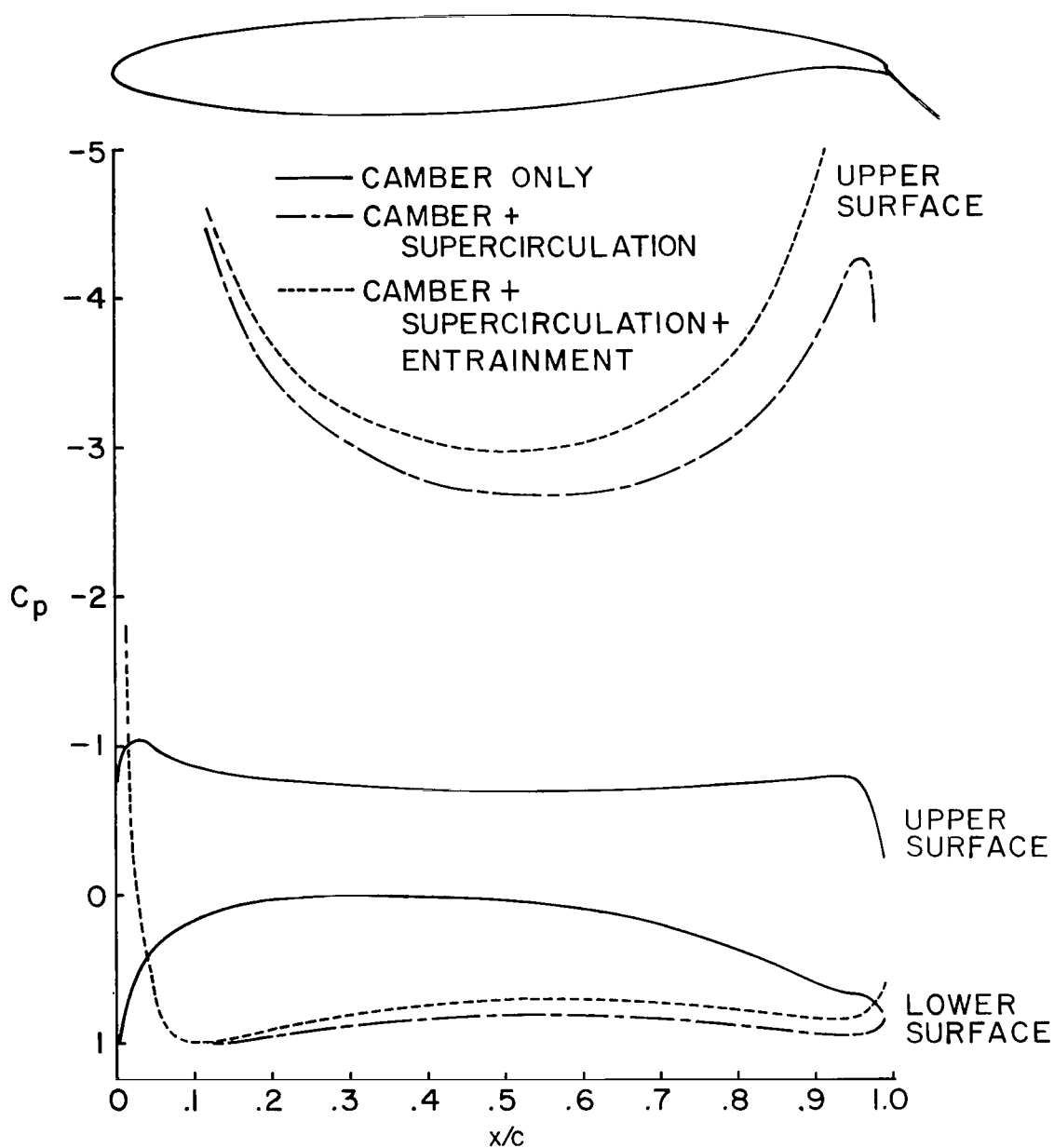


Figure 2.- Theoretical example demonstrating effects of supercirculation and entrainment on pressure distribution. $\tau = 45^\circ$; $C_j = 2.0$; thickness ratio = 0.13.

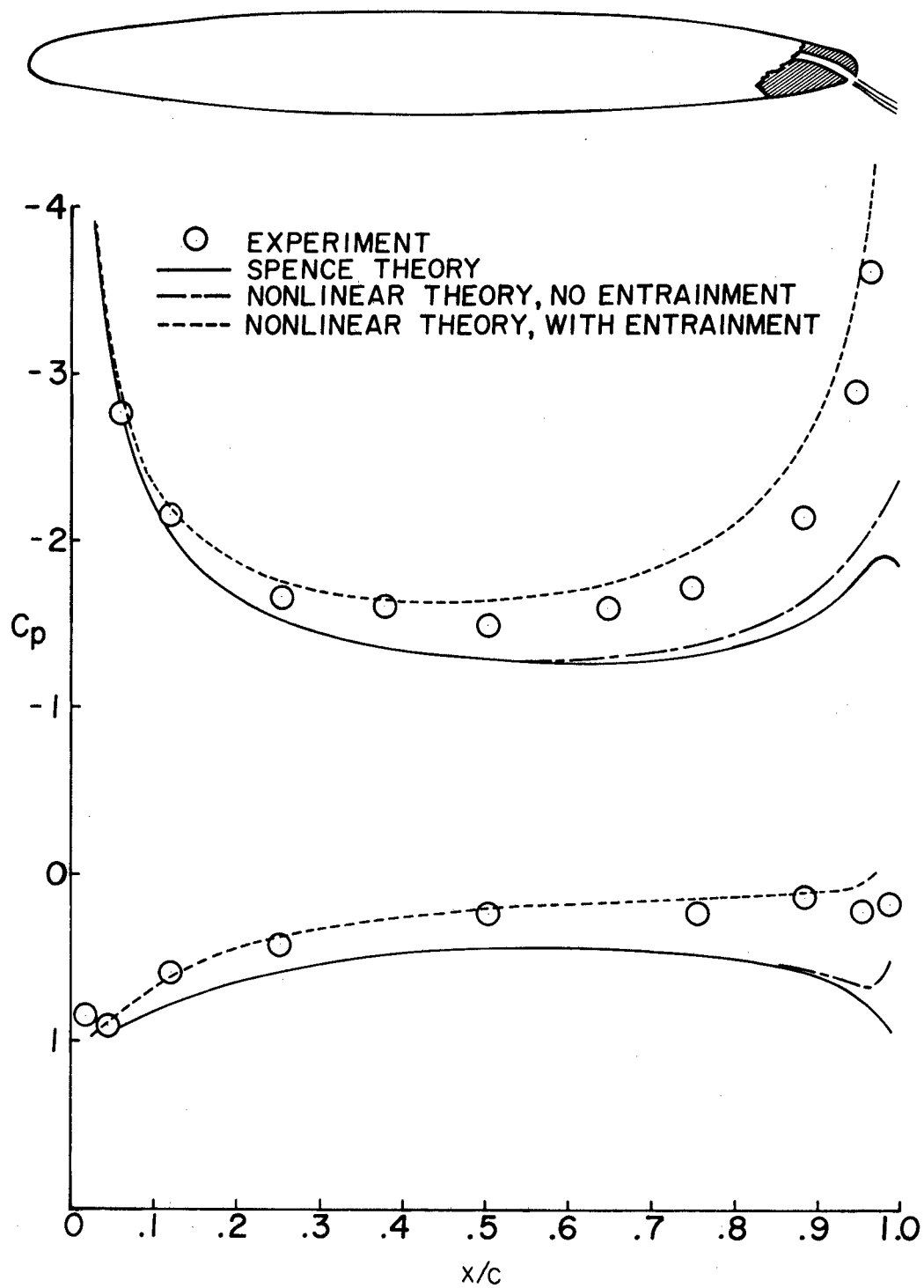


Figure 3.- Comparison of theories with experiment for elliptic profile.
Thickness ratio = 0.125; $C_j = 1.5$; $\tau = 31.4^\circ$.

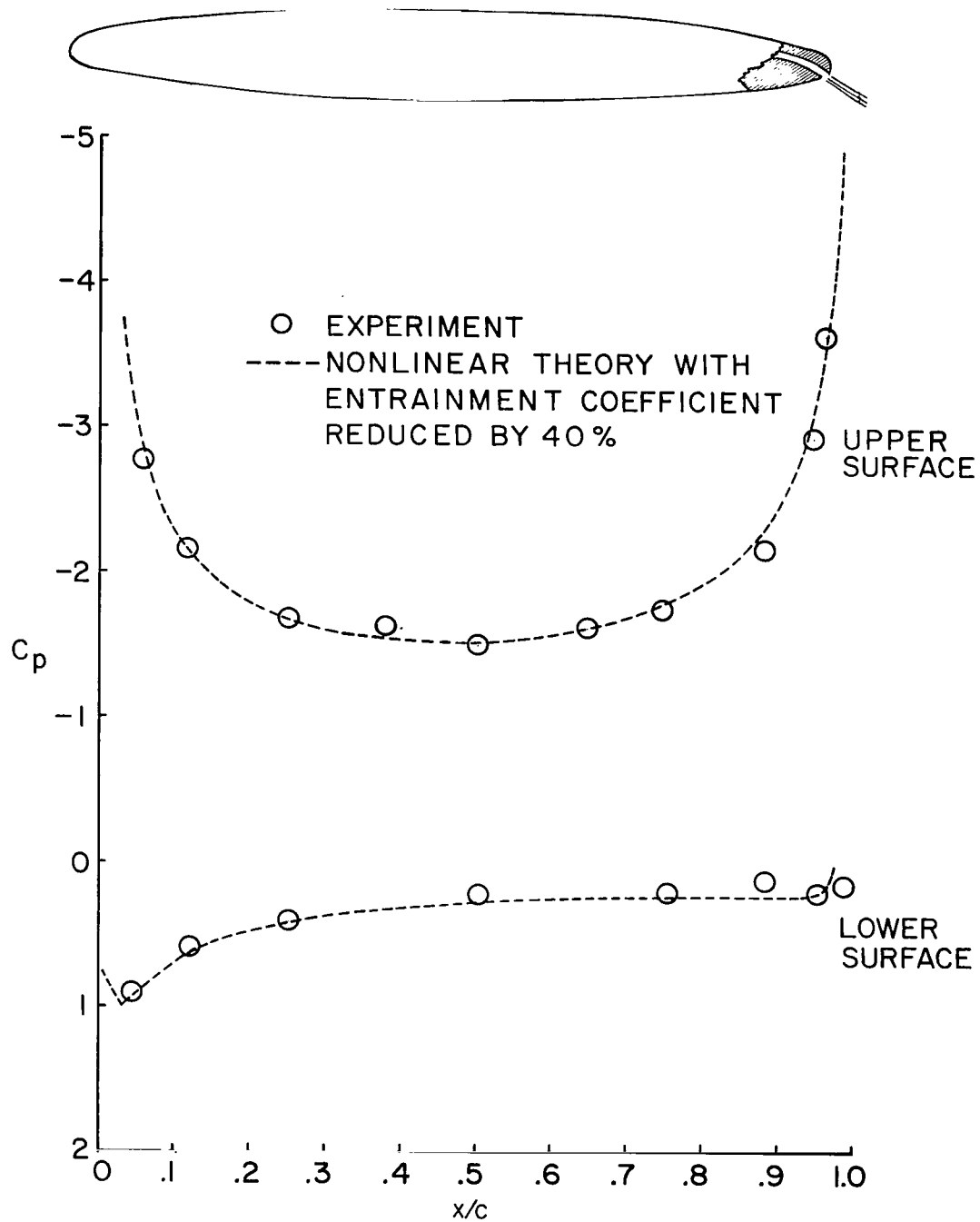


Figure 4.- Correlation of experiment with theoretical pressures (modified entrainment coefficient). Thickness ratio = 0.125; $C_j = 1.5$; $\tau = 31.4^\circ$.

NATIONAL AERONAUTICS AND SPACE ADMINISTRATION
WASHINGTON, D.C. 20546

OFFICIAL BUSINESS
PENALTY FOR PRIVATE USE \$300

SPECIAL FOURTH-CLASS RATE
BOOK

POSTAGE AND FEES PAID
NATIONAL AERONAUTICS AND
SPACE ADMINISTRATION
451



016 001 C1 U A 770107 S00903DS
DEPT OF THE AIR FORCE
AF WEAPONS LABORATORY
ATTN: TECHNICAL LIBRARY (SUL)
KIRTLAND AFB NM 87117

POSTMASTER: If Undeliverable (Section 158
Postal Manual) Do Not Return

"The aeronautical and space activities of the United States shall be conducted so as to contribute . . . to the expansion of human knowledge of phenomena in the atmosphere and space. The Administration shall provide for the widest practicable and appropriate dissemination of information concerning its activities and the results thereof."

—NATIONAL AERONAUTICS AND SPACE ACT OF 1958

NASA SCIENTIFIC AND TECHNICAL PUBLICATIONS

TECHNICAL REPORTS: Scientific and technical information considered important, complete, and a lasting contribution to existing knowledge.

TECHNICAL NOTES: Information less broad in scope but nevertheless of importance as a contribution to existing knowledge.

TECHNICAL MEMORANDUMS: Information receiving limited distribution because of preliminary data, security classification, or other reasons. Also includes conference proceedings with either limited or unlimited distribution.

CONTRACTOR REPORTS: Scientific and technical information generated under a NASA contract or grant and considered an important contribution to existing knowledge.

TECHNICAL TRANSLATIONS: Information published in a foreign language considered to merit NASA distribution in English.

SPECIAL PUBLICATIONS: Information derived from or of value to NASA activities. Publications include final reports of major projects, monographs, data compilations, handbooks, sourcebooks, and special bibliographies.

TECHNOLOGY UTILIZATION PUBLICATIONS: Information on technology used by NASA that may be of particular interest in commercial and other non-aerospace applications. Publications include Tech Briefs, Technology Utilization Reports and Technology Surveys.

Details on the availability of these publications may be obtained from:

SCIENTIFIC AND TECHNICAL INFORMATION OFFICE

NATIONAL AERONAUTICS AND SPACE ADMINISTRATION
Washington, D.C. 20546